HHS Public Access

Author manuscript

Stem Cells. Author manuscript; available in PMC 2015 August 04.

Published in final edited form as:

Stem Cells. 2010 November ; 28(11): 2053–2064. doi:10.1002/stem.524.

Adenomatous polyposis coli is essential for both neuronal differentiation and maintenance of adult neural stem cells in subventricular zone and hippocampus

Tetsuya Imura[#1], **Xiaohong Wang**[#1], **Tetsuo Noda**[2], **Michael V. Sofroniew**[3], and **Shinji Fushiki**[1]

[1]Department of Pathology and Applied Neurobiology, Graduate School of Medical Science, Kyoto Prefectural University of Medicine, Kyoto 602-8566, Japan

[2]Department of Cell Biology, The Cancer Institute, Japanese Foundation for Cancer Research, Tokyo 135-0063, Japan

[3]Department of Neurobiology, David Geffen School of Medicine, University of California, Los Angeles, Los Angeles, California 90095-1763.

[#] These authors contributed equally to this work.

Abstract

The tumor suppressor adenomatous polyposis coli (APC) is a multifunctional protein that not only inhibits the Wnt signaling pathway by promoting the degradation of beta-catenin but also controls cell polarity, motility, and division. APC is abundantly expressed in the adult central nervous system, but its role in adult neurogenesis remains unknown. Using conditional deletion (or knock-out) of APC (APC-CKO) from glial fibrillary acidic protein (GFAP)-expressing cells including adult neural stem cells (NSCs) in the subventricular zone and hippocampal dentate gyrus, we show that APC expression by these cells is a critical component of adult neurogenesis. Loss of APC function resulted in a marked reduction of GFAP-expressing NSC-derived new neurons, leading to the decreased volume of olfactory granule cell layer. Two distinct mechanisms account for impaired neurogenesis in APC-CKO mice. First, APC was highly expressed in migrating neuroblasts and APC deletion disturbed the differentiation from Mash1-expressing transient amplifying cells to neuroblasts with concomitant accumulation of beta-catenin. As a result, migrating neuroblasts decreased, whereas Mash1-expressing dividing cells reciprocally increased

Correspondence should be addressed to Tetsuya Imura, Department of Pathology and Applied Neurobiology, Graduate School of Medical Science, Kyoto Prefectural University of Medicine, Kawaramachi Hirokoji, Kamigyo-ku, Kyoto 602-8566, Japan, timura@koto.kpu-m.ac.jp.

Author Contribution

Tetsuya Imura: Conception and design, financial support, collection and/or assembly of data, data analysis and interpretation, manuscript writing, final approval of manuscript

Xiaohong Wang: Collection and/or assembly of data, data analysis and interpretation, final approval of manuscript

Tetsuo Noda: Provision of study material or patients, final approval of manuscript

Michael Sofroniew: Provision of study material or patients, data analysis and interpretation, manuscript writing, final approval of manuscript

Shinji Fushiki: Financial support, administrative support, data analysis and interpretation, manuscript writing, final approval of manuscript

Disclosure of Potential Conflicts of Interest

The authors indicate no potential conflicts of interest.

in the olfactory bulb of APC-CKO mice. Second, APC deletion promoted an exhaustion of the adult germinal zone. Functional NSCs and their progeny progressively depleted with age. These findings demonstrate that APC expression plays a key role in regulating intracellular beta-catenin level and neuronal differentiation of newly generated cells, as well as maintaining NSCs in the adult neurogenic niche.

Keywords

neurogenesis; neural stem cells; Wnt; beta-catenin; glial fibrillary acid protein

Introduction

Accumulating evidence suggests that adult neural stem cells (NSCs) not only play a role in certain aspects of physiological brain functions but also are involved in various pathological conditions including mood disorders, epilepsy, and tumorigenesis [1-3]. It is therefore of considerable interest to clarify the regulatory mechanisms in the behavior of adult NSCs. The canonical Wnt signaling pathway is one of the essential regulators of adult neurogenesis although its precise role has been the subject of some controversy [4-7]

The tumor suppressor adenomatous polyposis coli (APC) is a component of the canonical Wnt signaling pathway. Binding of Wnts to their receptor complex prevents the destruction of beta-catenin and induces its translocation into the nucleus to activate the transcription of target genes in association with the T-cell factor (Tcf)/lymphocyte enhancer factor (Lef) family. APC negatively regulates Wnt signaling by forming the beta-catenin destruction complex with axin and GSK-3beta, which is assumed as a critical part of its tumor suppressor function. Mutations in the APC gene have been identified in hereditary and sporadic human neoplastic conditions including brain tumors [8-11]. For instance, the patients having germline mutations in the APC gene occasionally develop medulloblastoma that supposedly originates from NSCs [12, 13]. In addition to the roles in Wnt signaling, APC binds to a variety of cytoskeletal components such as microtubules, EB1, Asef, and IQGAP1 to regulate cell polarity, motility, and division [10, 11]. Thus, APC is a multifunctional protein involved in various cellular events.

Despite its relatively ubiquitous expression, APC is particularly abundant both in the developing and adult central nervous system (CNS) including adult neurogenic regions [14, 15]. It has been shown that APC is involved in axon outgrowth, postsynaptic assembly, and glial migration [16-18], but the notions are largely based on *in vitro* studies. The homozygous APC null mutant embryos die before gastrulation [19] and the functions of APC in the adult CNS have not yet been directly examined *in vivo*. Given the expression pattern of APC in the adult CNS and its function as a component of the canonical Wnt pathway, we hypothesized that APC plays an important role in regulating adult neurogenesis. To test this hypothesis, we utilized the Cre/loxP system and APC^{580S} mice in which exon 14 of the APC gene is flanked by the two loxP sites. Cre-mediated recombination leads to a frameshift mutation at codon 580 and generates a C-terminally truncated protein lacking the binding domains for its major partners including beta-catenin,

axin, and microtubules. This strategy has been successfully applied to inactivate APC functions in different tissues [20-24]. In this study, we crossed mGFAP-Cre mice with APC^{580S} mice to ablate APC from postnatal NSCs.

Materials and Methods

Generation of APC-CKO mice

All APC-CKO and control mice were obtained from the same breeding colony of mGFAP-Cre mice of line 73.12 crossed with APC^{580S} mice on a C57BL/6 background. mGFAP-Cre mice were generated as described [25], using a 15 kb mouse GFAP promoter cassette (clone 445). mGFAP-Cre mice were cross-bred with APC^{580S} mice [20] to obtain mGFAP-Cre/$APC^{580S/580S}$ (APC-CKO) mice. Littermate mice carrying no mGFAP-Cre ($APC^{580S/+}$ and $APC^{580S/580S}$ mice) were used as controls unless otherwise noted. mGFAP-Cre mice were also cross-bred with the Cre enhanced green fluorescent protein (GFP) reporter mice kindly provided by Dr. Jun-ichi Miyazaki, Osaka University [26]. mGFAP-Cre/GFP/$APC^{580S/580S}$ mice are indicated as APC-CKO reporter mice and mGFAP-Cre/GFP/$APC^{+/+}$ mice from the same breeding colony are indicated as control reporter mice. Young adult mice (8-12 w) were used as 'adults' unless otherwise noted. Mice were housed in a temperature- and humidity-controlled SPF facility under a 12 h light/dark cycle with food and water available *ad libitum*. Experiments conducted according to protocols approved by the Committee for Animal Research, Kyoto Prefectural University of Medicine, Japan, and the animals were handled in accordance with the guidelines for the Care and Use of Laboratory Animals of Kyoto Prefectural University of Medicine.

PCR analysis

Genomic DNA was extracted using a DNeasy extraction kit (Qiagen) and both the undeleted and deleted alleles were amplified from 50 ng DNA using a combination of three primers; P3 (5'- GTTCTGTATCATGGAAAGATAGGTGGTC-3'), P4 (5'-CACTCAAAACGCTTTTGAGGGTTGATTC-3'), and P5 (5'-GAGTACGGGGTCTCTGTCTCAGTGAA-3'). P3 and P4 generate a 314bp PCR product corresponding to the loxP-flanked undeleted allele and P3 and P5 generate a 258bp product corresponding to the deleted allele by Cre-mediated recombination.

Histological procedures—BrdU (Sigma) was given as either a single i.p. injection of 200 mg/kg followed by perfusion with 4% paraformaldehyde after either 2 h or 48 hr, or six i.p. injections of 100 mg/kg every 12 h followed by perfusion after 14 d. Frozen sections were prepared using a cryostat microtome (Leica). In some cases, fixed tissues were embedded in paraffin and sectioned at 4 μm thickness with a microtome. Primary and secondary antibodies used for immunohistochemistry were in the supporting information Materials and Methods. Stained sections were examined and photographed using bright-field and fluorescence microscopy (Olympus) and scanning confocal laser microscopy (FV1000; Olympus). Stacks of 0.8-μm-thick optical slices were collected through the z-axis of tissue sections of regions to be analyzed. Only cells contained entirely within the three dimensions of a stack were analyzed.

Neurosphere culture

Multipotent neurospheres were generated from mouse periventricular zones as described previously [27, 28]. For quantitative analysis of neurosphere number, 10 days *in vitro* spheres were plated and counted (a minimum of three coverslips per condition). For differentiation, spheres were plated on poly-L-lysine-coated coverslips in the absence of growth factors for 5 d. For co-culture experiments, chimeric neurospheres were prepared from mixed single-cell suspensions of APC-CKO reporter cells (5000 cells/ml) and wild-type cells (10000 cells/ml). Differentiated cells were fixed and stained by immunocytochemistry with the primary antibodies listed above. For quantitative analysis, immunolabeled cells were counted (> 300 cells per coverslip and a minimum of three coverslips per condition).

Morphometric and statistical evaluation

The volume of olfactory bulb granule cell layer was measured according to the previously reported method with some modification [29], and are detailed in the supporting information Materials and Methods. The protocols for quantification of immunolabeled cells in the adult neurogenic regions *in vivo* and of neurite length *in vitro* are also described in the supporting information Materials and Methods. Values were shown as the mean + SEM and statistical evaluations were performed using Prism software (GraphPad).

Quantitative RT-PCR

Total RNA was isolated using an RNeasy extraction kit followed by DNase treatment (Qiagen). cDNA was synthesized from 2 μg of total RNA by SuperScript II reverse transcriptase (Invitrogen). Quantitative real-time PCR using the Sybr Green I reagent (Takara) was performed with ABI7000 (Applied Biosystems). The gene-specific primers used are described in the supporting information Materials and Methods. Primer Express software (Applied Biosystems) was used to design primers. Control experiments were performed without reverse transcriptase to ensure that the results were not due to amplifications of genomic DNA. PCR product identity was confirmed by electrophoresis and by melting-point analysis. A relative amount of transcript was estimated by the standard curve method. Three stable reference genes (beta2-microglobulin, Tbp, and Ywhaz) were selected from mouse housekeeping gene primer set (Takara) and the expression value of each gene was normalized using the geNorm software [30, 31].

Results

APC expression in the adult CNS

To investigate the roles of APC in adult neurogenesis, we took advantage of our previously established mouse line mGFAP-Cre 73.12. Adult mouse NSCs, but not embryonic NSCs, express GFAP [27, 32-34], and these mGFAP-Cre mice have been shown to target Cre activity and reporter gene expression selectively to postnatal and adult NSCs and their progeny in the hippocampus, subventricular zone (SVZ), and olfactory bulb (OB) [25] [35]. In this regard mGFAP-Cre mice differ from a commonly used hGFAP-Cre line that uses a 2.2kb fragment of the human GFAP promoter and non-specifically targets many

embryonically active radial progenitor cells that give rise to large populations of neurons through the brain [36]. We generated mGFAP-Cre/ $Apc^{580S/580S}$ (APC-CKO) mice by crossing mGFAP-Cre mice with APC^{580S} mice [20]. We first performed the PCR analysis to verify the specificity of Cre-mediated deletion of the APC gene. The genomic DNA isolated from $Apc^{580S/580S}$ mouse brains generated only the undeleted allele, whereas that from APC-CKO mouse brains generated both the deleted and undeleted alleles. Neither tail nor liver DNA of APC-CKO mice generated the deleted allele (*Supporting information Fig. 1A*). Thus the recombination is Cre-dependent as well as tissue-specific.

We next examined the distribution of APC in the forebrains of adult control and APC-CKO mice using the antibody against the C-terminal region of APC. APC-immunoreactivity (-IR) using this antibody has been shown to correlate well with the distribution of APC mRNA by *in situ* hybridization [15]. Intense APC-IR was identified in the outer plexiform layer of the OB and the molecular layer of the hippocampal dentate gyrus (DG) (*Fig. 1A, B*). APC-IR was also distributed in the dendrites/axons and neuronal somata in the CA1 region and cortices (*Fig. 1C, D, E*). In addition to neuronal localization, stellate-shaped APC-positive cells were scattered in the cortical gray matter and white matter (*Fig. 1D*). These cells were negative for astrocyte markers S100 and GFAP as well as the reporter GFP (*Fig. 1F, G, H*). These cells are likely to be oligodendrocyte lineage cells as previously reported [37] and are not the target of Cre-mediated recombination in this model.

In the adult neurogenic regions including the SVZ, the rostral migratory stream (RMS), and the OB, clusters of small cells exhibited strong APC-IR (*Fig. 1I, K, M*). APC-positive cells were also positive for a neuroblast marker PSA-NCAM, but negative for a putative stem cell marker GFAP and a transient amplifying cell (TAC) marker Mash1 (*Fig. 1Q, R, S*). In APC-CKO mice, APC-IR was markedly reduced in these regions, whereas APC-IR outside the neurogenic regions was well preserved (*Fig. 1J, L, N)*. APC-IR was also abundant in the dendrites of granule cells in the DG, another neurogenic region. APC-CKO mice, however, displayed no obvious reduction in APC-IR (*Fig. 10, P)*. This is likely due to the lower contribution of GFAP-expressing NSCs to this region compared to the OB (*see the next section*).

These results demonstrate that neuroblasts abundantly express APC in the adult neurogenic regions and APC expression is selectively ablated from these regions in APC-CKO mice.

Phenotypes of APC-CKO mice

APC-CKO mice were born at the expected Mendelian ratio, indicating no embryonic lethality. Approximately 25% of APC-CKO mice, however, exhibited severe growth retardation postnatally and died by 8 weeks due to hemorrhagic enteritis (*Supporting information Fig. 1B, C, D*). These mice also showed a “small eye” phenotype with lens dysmorphogenesis (*Supporting information Fig. 1E*). These non-CNS phenotypes were caused by loss of APC in GFAP-positive enteric glia and lens epithelium [24, 38-40], and will be described in detail elsewhere. The rest of APC-CKO mice showed much milder non-CNS phenotypes. It is unlikely that this variation was due to a different degree of Cre-loxP recombination between individuals since the recombination efficiency monitored by the Cre reporter as well as the CNS phenotypes described below were similar regardless of non-CNS

phenotypes (*data not shown*). Nevertheless, we excluded the mice with severe gut and eye phenotypes from the study afterwards because of their vulnerability and lethality.

Brain weights from adult APC-CKO and littermate control mice (8-12w) were not significantly different (0.41 ± 0.036g in CKO vs. 0.43 ± 0.027g in controls). The macroscopic appearance of APC-CKO mouse brains was normal except for the small OB. The volume of the olfactory granule cell layer (OB-GCL) was reduced by 38% (*Fig. 2A*). Although APC should also be deleted in astrocytes, we found no obvious histological abnormality in GFAP-positive and S100-positive astrocytes in the forebrains of APC-CKO mice (*Fig. 2B*). It is unlikely that astrocytes escaped from Cre-mediated recombination since they broadly expressed GFP in APC-CKO reporter mice (*see below*).

The shrunken OB-GCL raises the possibility that APC deletion disturbs GFAP-expressing NSC-derived neurogenesis. We therefore determined the overall contribution of GFAP-expressing NSCs to the two adult neurogenic regions using the Cre reporter mice. In control reporter mice, 64% of total NeuN-positive neurons were GFP-positive in the OB-GCL, whereas 20% were GFP-positive in the DG-GCL (*Fig. 2C*). Thus, the overall contribution of GFAP-expressing NSCs to the OB-GCL is much higher, which is consistent with the recent reports [25, 41]. In APC-CKO reporter mice, the proportion of GFP-positive neurons markedly decreased to 17% and 6% in the OB-GCL and DG-GCL, respectively (*Fig. 2C*). These findings indicate that APC deletion disturbs GFAP-expressing NSC-derived neurogenesis, resulting in a significant volume reduction in OB-GCL.

Depletion of neuroblasts with a concomitant increase in Mash1-expressing dividing cells in the OB of APC-CKO mice

To investigate the mechanisms in reduced neurogenesis in APC-CKO mice, we first quantified cell proliferation by 2 hr BrdU pulse labeling. The number of BrdU-incorporated cells in the SVZ of APC-CKO mice decreased by 62% compared to controls, demonstrating the suppression of SVZ cell proliferation (*Fig. 3A, B*). The number of BrdU-positive cells rostrally declined in controls, indicating that newly generated cells exit cell cycle as they proceed to the OB. Interestingly, this caudorostral gradient of BrdU-positive cells was disturbed in APC-CKO mice. In contrast to the reduction in SVZ cell proliferation, the number of BrdU-positive cells was comparable in the rostral RMS (82% of controls) and was more than 9 times higher in the OB (*Fig. 3A, B*). This increased BrdU incorporation did not reflect DNA damage/repair since Ki67, another independent marker for cell proliferation, also increased (*Fig. 3B*).

We next examined the cellular compositions of the SVZ, RMS, and OB of APC-CKO mice. In the SVZ, GFAP expression was indistinguishable, the number of Mash1-positive TACs was slightly fewer (86% of controls), and that of Dcx-positive neuroblasts significantly reduced (35% of controls) (*Fig. 3A, B).* In controls, the number of Mash1-positive cells rostrally declined and Dcx-positive cells become predominant, reflecting the maturation of newly generated cells. In APC-CKO mice, the number of Mash1-positive cells slightly increased in the RMS (110% and 130% of controls in the caudal and rostral RMS, respectively) and was more than 50 times higher in the OB (*Fig. 3A, B*). On the other hand, the number of Dcx-positive cells markedly decreased (25%, 21%, 7% of controls in the

caudal RMS, rostral RMS, and OB, respectively). To exclude the possibility that APC deletion just downregulates Dcx expression, we also analyzed the expression of another neuroblast marker PSA-NCAM and found that PSA-NCAM-positive cells similarly decreased (*Fig. 3B*). The majority of BrdU-positive dividing cells ectopically increased in the OB were GFP positive (78%, 130/167 cells, n=3) but negative for astrocyte markers (*Fig. 3C*), indicating that they are not dividing astrocytes but the progeny of GFAP-expressing NSCs. Only a few cells expressed Dcx (4%, 9 per 202 cells, n=4) and Olig2 (9%, 20/219 cells, n=4). On the other hand, 67% of BrdU-positive cells were Mash1-positive (177/264 cells, n=4)(*Fig. 3C*). Therefore, we conclude that Mash1-expressing cells originating from GFAP-expressing NSCs comprise the majority of dividing cells in the OB of APC-CKO mice.

Fate of newly generated cells in APC-CKO mice

We next determined the fate of newly generated cells. In controls, a number of BrdU-positive cells migrated into the OB-GCL and 74% were differentiated into NeuN-positive neurons at 14 d after the last BrdU injection (155/210 cells, n=4, *Fig. 4A, B*). In APC-CKO mice, only a few BrdU-positive cells were identified in the OB-GCL (5.4% of controls). Most of BrdU-positive cells still remained in the SVZ and RMS, and the number of them was rather higher (160%, 151%, and 253% of controls in the SVZ, caudal RMS, and OB-RMS, respectively). BrdU-positive cells remaining in the RMS were negative for NeuN and only a few of them were positive for neuronal/glial markers Dcx (8%, 22/284 cells, n=4), GFAP (5%, 14/262 cells, n=4), and S100 (3%, 6/240 cells, n=4). Some expressed immature progenitor markers Mash1 (26%, 63/240 cells, n=4), Olig2 (14%, 36/258 cells, n=4), and Pax6 (10%, 17/165 cells, n=3) (*Fig. 4B, C)*. Thus, newly generated cells failed to reach their final destination and differentiate into a mature neuronal phenotype. Most of the cells remaining in the RMS either stayed an immature stage or acquired an unknown phenotype. This notion is further supported by the finding that BrdU-incorporated cells at 48 hr after BrdU administration remained Dcx-negative in APC-CKO mice, whereas the majority of them were already Dcx-positive in controls (*Fig. 4D*). We also examined if impaired differentiation and migration of newly generated cells are coupled with increased cell death. The number of cells undergoing apoptosis, as detected by cleaved caspase-3, did not significantly differ outside the neurogenic regions (*data not shown*). On the other hand, the number of caspase-3-positive cells significantly increased in the SVZ, caudal RMS, and OB of APC-CKO mice (330%, 686%, and 375% of controls, respectively, *Fig. 4E*).

Accumulation of beta-catenin and aberrant cell aggregation in APC-CKO mice

To study the consequence of APC deletion for the Wnt/beta-catenin signaling pathway, we next examined the distribution and accumulation of beta-catenin. Beta-catenin was modestly expressed in the neurogenic regions of control mice and predominantly localized in cell-cell boundaries. Only a few cells exhibited weak cytoplasmic and nuclear staining. On the other hand, beta-catenin expression markedly increased in APC-CKO mice. Strong beta-catenin-IR was localized in both the cytoplasm and nucleus (*Fig. 4F*). Most of Mash1-positive dividing cells in the SVZ and RMS exhibited a marked accumulation of beta-catenin. In contrast, no detectable increase in beta-catenin-IR was observed in Dcx-positive and GFAP-positive cells (*Fig. 4G*).

We also examined the distribution and morphology of the reporter GFP-positive cells. In the RMS of control reporter mice, GFP-positive cells were orderly arranged in a caudorostral orientation known as “tangential chain-like migration’ [42]. The vast majority of them were Dcx-positive neuroblasts. In APC-CKO reporter mice, not only the number of Dcx-positive cells decreased but also the remaining Dcx-positive cells lost their organized arrangement and randomly dispersed. In addition, GFP-positive Dcx-negative cells frequently formed small cell aggregates (*Fig. 4H*). The cell aggregates were tightly packed and accumulated beta-catenin. Mash1-positive cells were found within these aggregates. Outside the neurogenic regions, no beta-catenin accumulation was identified in astrocytes even though they broadly expressed GFP (*Fig. 4I*).

These findings thus demonstrate that APC deletion from GFAP-expressing NSCs results in the accumulation of beta-catenin at the stage of Mash1-expressing TACs, concomitant with the formation of aberrant cell aggregates.

Aberrant neuronal differentiation of APC-CKO progenitors in vitro

We next evaluated the effects of APC deletion on the differentiation potential of NSCs *in vitro* using the neurosphere culture system. The proportions of GFAP-positive astrocytes and O4-positive oligodendrocytes differentiated were not significantly different and the cellular morphologies were indistinguishable between control and APC-CKO cultures (*Fig. 5A*). On the other hand, the proportion of Tuj1-positive cells in APC-CKO cultures significantly increased by 50%, but their morphology was drastically altered. They had spherical somata with either short fat neurites or no identifiable neurite (87% reduction compared to control cultures) (*Fig. 5A, B*).

Morphologically abnormal Tuj1-positive cells frequently formed tightly packed cell clusters and accumulated beta-catenin, which is similar to the cell aggregates observed *in vivo* (*Fig. 5C*). The expression of Axin2 mRNA, an indicator of beta-catenin-mediated transcription, markedly increased in APC-CKO cells (11.6-fold increase, *Fig. 5D*). We also examined the expression of other neuronal markers and the genes regulating neuronal differentiation. Almost all Tuj1-positive cells were Dcx-positive but Mash1-negative in control cultures. In contrast, Tuj1-positive cells in APC-CKO cultures expressed neither Dcx nor PSA-NCAM, whereas they occasionally expressed Mash1 (*Fig. 5E*). They never expressed glial markers including Olig2, O4, and GFAP (*data not shown*). Thus, morphologically abnormal Tuj1-positive cells are likely to be neuronal lineage cells. The expression of Mash1 mRNA significantly increased (165% of controls), whereas that of Dlx2 and NeuroD1 mRNA, neuronal differentiation genes, contrarily decreased (41% and 55% of controls, *Fig. 5F*). These results suggest that APC deletion does not prevent the induction of neuronal fate but disturbs the proper differentiation/maturation of new neurons.

It remains possible that neuronal differentiation/maturation is impaired due to loss of supportive functions of APC-deficient non-neuronal cells such as astrocytes. To test this possibility, we also performed the co-culture of wild-type cells and APC-CKO reporter cells. Despite the presence of non-neuronal wild-type cells, Tuj1-positive APC-deficient cells exhibited the same abnormal morphology, whereas GFP-negative wild-type neurons

remained normal (*Fig. 5G*). This indicates that the impaired neuronal differentiation observed here is the cell-autonomous effect of APC deletion.

Progressive depletion of adult germinal zone in APC-CKO mice

Even though our results so far show that the transition from Mash1-positive TACs to neuroblasts was disturbed, there was no increase in Mash1-positive dividing cells in the SVZ of young adult APC-CKO mice. One possibility is that the number of functional NSCs decreases to mask an increase in Mash1-positive cells. To address this question, we first propagated NSCs as a sphere-forming colony from the periventricular tissues of postnatal day 4 (P4), young adult (8-12w), and middle-aged (6-7 month) mice. We have previously shown that essentially all neurospheres originate from GFAP-expressing NSCs at these ages [27]. The number of primary neurospheres generated from APC-CKO mice was significantly lower compared to that from age-matched control mice at all ages examined, but it progressively declined with age (63%, 25%, and 9% of controls at P4, young adult, and middle-aged, respectively, *Fig. 6A*). We were unable to passage neurospheres from middle-aged APC-CKO mice because of its very low yield, but we were able to generate secondary and tertiary spheres from P4 and young adult APC-CKO mice. The number of tertiary spheres generated from the same plating density was still significantly lower but improved (74%, and 62% of controls at P4 and young adult, respectively, *Fig. 6A*). This improvement was not the rescue effect that a few cells escaping from Cre-mediated recombination grew to replace APC-CKO cells since the tertiary spheres contained very few APC but abundantly expressed GFP (*data not shown*). The yield of tertiary spheres was comparable between P4 and young adult APC-CKO spheres. These findings indicate that cell proliferation is similarly impaired *in vitro* in APC-CKO mice regardless of age. A progressive reduction in primary neurosphere number with age is likely to reflect a decrease in the number of neurosphere-initiating cells.

We next examined the cellular compositions and cell proliferation in the SVZ of middle-aged APC-CKO mice that exhibited a very low yield of primary neurospheres. The number of BrdU(2 h)-positive dividing cells as well as Dcx-positive neuroblasts markedly decreased (12% and 11% of controls, respectively), which is further exacerbated from younger age. Moreover, the number of Mash1-positive cells significantly decreased at this age (30% of controls, *Fig. 6B, C*). GFAP-immunoreactivity also moderately decreased (*Fig. 6C*). In the OB, beta-catenin-accumulated cells as well as BrdU-positive dividing cells were still identified but attenuated compared to younger age (*Fig. 6D*). These results show that functional NSCs and their progeny progressively deplete in APC-CKO mice with age.

Reduced hippocampal neurogenesis with relatively spared cell proliferation

We next studied neurogenesis in the DG to examine if the different consequences occur by APC deletion [43]. Cell proliferation in the DG of young adult APC-CKO mice modestly decreased (70% of controls, *Fig. 7A*) but relatively spared compared to the SVZ. GFAP expression in the subgranular zone (SGZ) was indistinguishable, but Dcx-positive neuroblasts markedly decreased (*Fig. 7B*). Thus, despite a mild decrease in cell genesis neuroblasts were severely depleted. We also examined the fate of newly generated cells. The total number of BrdU-positive cells (14 d) mildly but not significantly decreased (82% of

controls), which is approximately proportional to the reduction in cell proliferation. 31% of BrdU-positive cells were differentiated into NeuN-positive neurons in control mice at this time point. In contrast, only 5% were NeuN-positive in APC-CKO mice and the majority of BrdU-positive but NeuN-negative cells remained in the SGZ (*Fig. 7C*). They expressed GFP, indicating that they are the progeny of GFAP-expressing NSCs. Similar to those observed in the SVZ-OB, tightly packed cell aggregates with beta-catenin accumulation resided along the SGZ. A few isolated GFP-positive cells in the hilus and GCL extended processes, but these processes were disorganized and randomly directed (*Fig. 7D*).

These findings show that APC deletion impairs the production of neuroblasts with relatively spared cell genesis in the DG. Newly generated cells fail to pursue their normal differentiation pathway and form aberrant cell aggregates with beta-catenin accumulation, which is similar to the effects of APC deletion on SVZ NSCs.

Discussion

In the present study, we determined if the tumor suppressor APC plays a critical role in regulating adult neurogenesis by using conditional gene targeting in mice. Our results demonstrate that APC deletion from GFAP-expressing NSCs disrupts postnatal and adult neurogenesis by the following mechanisms; 1) Differentiation from Mash1-expressing TACs to neurons is impaired with concomitant beta-catenin accumulation and its target gene activation. 2) Adult NSCs and their neurogenic niche are progressively depleted with age.

Although mouse 15kb GFAP promoter we used, unlike human GFAP promoter, selectively directs expression only to postnatal GFAP-expressing NSCs, there are still two methodological considerations. First, it has been suggested that both GFAP-positive and -negative NSCs coexist in the adult SVZ [44] and this promoter therefore fails to cover all NSC population. Nevertheless, we have previously shown that more than 95% of new neurons in the adult OB are derived from the cells in which this promoter is active [25]. This indicates that GFAP-negative NSCs, if any, either transit to a GFAP-positive state to generate new neurons or contribute little to basal neurogenesis. Second, GFAP is not a specific marker for NSCs and this promoter also directs expression to astrocytes as well as GFAP-expressing cells outside the CNS [35, 38]. Indeed, APC-CKO mice unexpectedly exhibited gut and eye phenotypes, indicating the importance of APC in these organs. On the other hand, we found no obvious change in the distribution and morphology of APC-deficient forebrain astrocytes. APC expression was below detectable levels in astrocytes in the forebrain of control mice and beta-catenin accumulation was not induced by APC deletion. However, it remains possible that APC plays a role in certain aspects of astrocyte function or in specific populations of astrocytes. Reactive astrocytes are shown to upregulate APC [45]. An *in vitro* study has reported that APC regulates the migration of astrocytes [16].

Despite these limitations, we conclude that cell-autonomous mechanisms in postnatal NSCs largely contribute to the impaired neuronal differentiation in APC-CKO mice observed here. CNS phenotypes were consistent regardless of the severity of non-CNS phenotypes. Impaired neuronal differentiation was partly reproduced *in vitro* and was not rescued by the

support of wild-type cells. Moreover, the transition from Mash1-positive TACs to neuroblasts was disrupted in association with intracellular accumulation of beta-catenin. Although Mash1-positive TACs also generate oligodendrocytes [46, 47], only a small portion of newly generated cells along the RMS of APC-CKO mice expressed Olig2, a marker for glial progenitor cells and oligodendrocytes. In addition, we found no obvious increase in Mash1 and Olig2-positive cells in the corpus callosum where adult NSC-derived oligodendrocyte progenitors migrate (*data not shown*). It is therefore likely that APC deletion impairs neuronal differentiation without changing cell fate.

There are two possible molecular mechanisms in regulating neuronal differentiation by APC; beta-catenin-dependent and –independent pathways. We assume that beta-catenin-dependent pathway is the major cause of impaired neuronal differentiation. Neuroblasts highly expressed APC and APC deletion resulted in beta-catenin accumulation in Mash1-positive TACs. Such a reciprocal pattern of beta-catenin and APC expression is observed in normal brain development. Beta-catenin is downregulated but APC is upregulated as cells exit ventricular zone and differentiate into postmitotic neurons [14, 21, 48]. Moreover, transduction of stabilized beta-catenin inhibits the differentiation of Mash1-expressing TACs to neuroblasts in the adult SVZ [49]. It is thus reasonable to propose that APC promotes the transition from TACs to neuroblasts by reducing intracellular beta-catenin level. The promoter regions of several key transcription factors for neurogenesis, including Mash1, contain the binding element for a beta-catenin/Tcf complex [50]. Precise regulation of intracellular beta-catenin level by APC may determine the timing of expression of these factors. In this regard, it will be interesting to see if APC overexpression in TACs decreases beta-catenin and induces premature neuronal differentiation. However, it remains possible that beta-catenin-independent pathways are involved. APC acts as a microtubule-binding protein to regulate neural cell polarity, adhesion, migration, and neurite outgrowth. The orientation of migrating neuroblasts was disorganized and aberrant cell aggregates frequently formed *in vivo*, and neurite outgrowth was severely impaired *in vitro* These phenotypes could be attributed to misregulation of microtubules as previously indicated [18, 22]. Both possibilities are not mutually exclusive and APC may play multiple roles in neuronal differentiation via different pathways.

Contrary to our expectation, APC deletion suppressed SVZ cell proliferation, leading to increased levels of apoptosis and progressive exhaustion of neurogenic pool. This is similar to the effects of APC deletion on embryonic neurogenesis [21, 22], but in sharp contrast to the observations that stabilized beta-catenin increases neural progenitor proliferation both during development and in adults [49, 51-53]. The most plausible explanation for the discrepancy is that loss of beta-catenin independent functions of APC counteracts the effects of Wnt/beta-catenin signaling activation. For example, APC regulates chromosome segregation during mitosis by binding microtubules, and loss of APC induces chromosomal abnormalities [54, 55]. APC deletion from GFAP-expressing NSCs may disrupt efficient cell division, leading to progressive elimination of damaged NSCs and their progeny [56, 57].

In summary, our results implicate APC in promoting neuronal differentiation and maintaining NSCs in the adult neurogenic niche. APC is particularly important in

controlling intracellular beta-catenin level upon the transition from TACs to neuroblasts, providing insight into the roles and regulation of the canonical Wnt pathway in adult neurogenesis.

Supplementary Material

Refer to Web version on PubMed Central for supplementary material.

Acknowledgements

This work was supported by grants-in-aid from the Ministry of Education, Culture, Sports, Science and Technology of Japan (18500245) and fellowships from the Rotary Yoneyama Memorial Foundation (X.W.) and National Institutes of Health USA, NINDS NS057624 (M.V.S). The authors thank to M. Tominaga for technical assistance.

References

1. Vescovi AL, Galli R, Reynolds BA. Brain tumour stem cells. Nat Rev Cancer. 2006; 6:425–36. [PubMed: 16723989]
2. Zhao C, Deng W, Gage FH. Mechanisms and functional implications of adult neurogenesis. Cell. 2008; 132:645–60. [PubMed: 18295581]
3. Parent JM. Adult neurogenesis in the intact and epileptic dentate gyrus. Prog Brain Res. 2007; 163:529–40. [PubMed: 17765736]
4. Kalani MY, Cheshier SH, Cord BJ, et al. Wnt-mediated self-renewal of neural stem/progenitor cells. Proc Natl Acad Sci U S A. 2008; 105:16970–5. [PubMed: 18957545]
5. Lie DC, Colamarino SA, Song HJ, et al. Wnt signalling regulates adult hippocampal neurogenesis. Nature. 2005; 437:1370–5. [PubMed: 16251967]
6. Wexler EM, Paucer A, Kornblum HI, et al. Endogenous Wnt signaling maintains neural progenitor cell potency. Stem Cells. 2009; 27:1130–41. [PubMed: 19418460]
7. Michaelidis TM, Lie DC. Wnt signaling and neural stem cells: caught in the Wnt web. Cell Tissue Res. 2008; 331:193–210. [PubMed: 17828608]
8. Kinzler KW, Nilbert MC, Su LK, et al. Identification of FAP locus genes from chromosome 5q21. Science. 1991; 253:661–5. [PubMed: 1651562]
9. Nishisho I, Nakamura Y, Miyoshi Y, et al. Mutations of chromosome 5q21 genes in FAP and colorectal cancer patients. Science. 1991; 253:665–9. [PubMed: 1651563]
10. Aoki K, Taketo MM. Adenomatous polyposis coli (APC): a multi-functional tumor suppressor gene. J Cell Sci. 2007; 120:3327–35. [PubMed: 17881494]
11. Nathke IS. The adenomatous polyposis coli protein: the Achilles heel of the gut epithelium. Annu Rev Cell Dev Biol. 2004; 20:337–66. [PubMed: 15473844]
12. Rossi A, Caracciolo V, Russo G, et al. Medulloblastoma: from molecular pathology to therapy. Clin Cancer Res. 2008; 14:971–6. [PubMed: 18281528]
13. Sutter R, Shakhova O, Bhagat H, et al. Cerebellar stem cells act as medulloblastoma-initiating cells in a mouse model and a neural stem cell signature characterizes a subset of human medulloblastomas. Oncogene. 2010; 29:1845–56. [PubMed: 20062081]
14. Bhat RV, Baraban JM, Johnson RC, et al. High levels of expression of the tumor suppressor gene APC during development of the rat central nervous system. J Neurosci. 1994; 14:3059–71. [PubMed: 8182459]
15. Brakeman JS, Gu SH, Wang XB, et al. Neuronal localization of the Adenomatous polyposis coli tumor suppressor protein. Neuroscience. 1999; 91:661–72. [PubMed: 10366023]
16. Etienne-Manneville S, Hall A. Cdc42 regulates GSK-3beta and adenomatous polyposis coli to control cell polarity. Nature. 2003; 421:753–6. [PubMed: 12610628]
17. Temburni MK, Rosenberg MM, Pathak N, et al. Neuronal nicotinic synapse assembly requires the adenomatous polyposis coli tumor suppressor protein. J Neurosci. 2004; 24:6776–84. [PubMed: 15282282]

18. Zhou FQ, Zhou J, Dedhar S, et al. NGF-induced axon growth is mediated by localized inactivation of GSK-3beta and functions of the microtubule plus end binding protein APC. Neuron. 2004; 42:897–912. [PubMed: 15207235]
19. Oshima M, Oshima H, Kitagawa K, et al. Loss of Apc heterozygosity and abnormal tissue building in nascent intestinal polyps in mice carrying a truncated Apc gene. Proc Natl Acad Sci U S A. 1995; 92:4482–6. [PubMed: 7753829]
20. Shibata H, Toyama K, Shioya H, et al. Rapid colorectal adenoma formation initiated by conditional targeting of the Apc gene. Science. 1997; 278:120–3. [PubMed: 9311916]
21. Ivaniutsin U, Chen Y, Mason JO, et al. Adenomatous polyposis coli is required for early events in the normal growth and differentiation of the developing cerebral cortex. Neural Develop. 2009; 4:3.
22. Yokota Y, Kim WY, Chen Y, et al. The adenomatous polyposis coli protein is an essential regulator of radial glial polarity and construction of the cerebral cortex. Neuron. 2009; 61:42–56. [PubMed: 19146812]
23. Colnot S, Decaens T, Niwa-Kawakita M, et al. Liver-targeted disruption of Apc in mice activates beta-catenin signaling and leads to hepatocellular carcinomas. Proc Natl Acad Sci U S A. 2004; 101:17216–21. [PubMed: 15563600]
24. Martinez G, Wijesinghe M, Turner K, et al. Conditional mutations of beta-catenin and APC reveal roles for canonical Wnt signaling in lens differentiation. Invest Ophthalmol Vis Sci. 2009; 50:4794–806. [PubMed: 19515997]
25. Garcia AD, Doan NB, Imura T, et al. GFAP-expressing progenitors are the principal source of constitutive neurogenesis in adult mouse forebrain. Nat Neurosci. 2004; 7:1233–41. [PubMed: 15494728]
26. Kawamoto S, Niwa H, Tashiro F, et al. A novel reporter mouse strain that expresses enhanced green fluorescent protein upon Cre-mediated recombination. FEBS Lett. 2000; 470:263–8. [PubMed: 10745079]
27. Imura T, Kornblum HI, Sofroniew MV. The predominant neural stem cell isolated from postnatal and adult forebrain but not early embryonic forebrain expresses GFAP. J Neurosci. 2003; 23:2824–32. [PubMed: 12684469]
28. Imura T, Nakano I, Kornblum HI, et al. Phenotypic and functional heterogeneity of GFAP-expressing cells in vitro: differential expression of LeX/CD15 by GFAP-expressing multipotent neural stem cells and non-neurogenic astrocytes. Glia. 2006; 53:277–93. [PubMed: 16267834]
29. Petreanu L, Alvarez-Buylla A. Maturation and death of adult-born olfactory bulb granule neurons: role of olfaction. J Neurosci. 2002; 22:6106–13. [PubMed: 12122071]
30. Vandesompele J, De Preter K, Pattyn F, et al. Accurate normalization of real-time quantitative RT-PCR data by geometric averaging of multiple internal control genes. Genome Biol. 2002; 3:34.1–34.11.
31. Coulson DT, Brockbank S, Quinn JG, et al. Identification of valid reference genes for the normalization of RT qPCR gene expression data in human brain tissue. BMC Mol Biol. 2008; 9:46. [PubMed: 18460208]
32. Laywell ED, Rakic P, Kukekov VG, et al. Identification of a multipotent astrocytic stem cell in the immature and adult mouse brain. Proc Natl Acad Sci U S A. 2000; 97:13883–8. [PubMed: 11095732]
33. Seri B, Garcia-Verdugo JM, McEwen BS, et al. Astrocytes give rise to new neurons in the adult mammalian hippocampus. J Neurosci. 2001; 21:7153–60. [PubMed: 11549726]
34. Doetsch F, Caille I, Lim DA, et al. Subventricular zone astrocytes are neural stem cells in the adult mammalian brain. Cell. 1999; 97:703–16. [PubMed: 10380923]
35. Herrmann JE, Imura T, Song B, et al. STAT3 is a critical regulator of astrogliosis and scar formation after spinal cord injury. J Neurosci. 2008; 28:7231–43. [PubMed: 18614693]
36. Zhuo L, Theis M, Alvarez-Maya I, et al. hGFAP-cre transgenic mice for manipulation of glial and neuronal function in vivo. Genesis. 2001; 31:85–94. [PubMed: 11668683]
37. Bhat RV, Axt KJ, Fosnaugh JS, et al. Expression of the APC tumor suppressor protein in oligodendroglia. Glia. 1996; 17:169–74. [PubMed: 8776583]

38. Bush TG, Savidge TC, Freeman TC, et al. Fulminant jejuno-ileitis following ablation of enteric glia in adult transgenic mice. Cell. 1998; 93:189–201. [PubMed: 9568712]
39. Hatfield JS, Skoff RP, Maisel H, et al. Glial fibrillary acidic protein is localized in the lens epithelium. J Cell Biol. 1984; 98:1895–8. [PubMed: 6373785]
40. Boyer S, Maunoury R, Gomes D, et al. Expression of glial fibrillary acidic protein and vimentin in mouse lens epithelial cells during development in vivo and during proliferation and differentiation in vitro: comparison with the developmental appearance of GFAP in the mouse central nervous system. J Neurosci Res. 1990; 27:55–64. [PubMed: 2254956]
41. Imayoshi I, Sakamoto M, Ohtsuka T, et al. Roles of continuous neurogenesis in the structural and functional integrity of the adult forebrain. Nat Neurosci. 2008; 11:1153–61. [PubMed: 18758458]
42. Alvarez-Buylla A, Garcia-Verdugo JM. Neurogenesis in adult subventricular zone. J Neurosci. 2002; 22:629–34. [PubMed: 11826091]
43. Bull ND, Bartlett PF. The adult mouse hippocampal progenitor is neurogenic but not a stem cell. J Neurosci. 2005; 25:10815–21. [PubMed: 16306394]
44. Chojnacki AK, Mak GK, Weiss S. Identity crisis for adult periventricular neural stem cells: subventricular zone astrocytes, ependymal cells or both? Nat Rev Neurosci. 2009; 10:153–63. [PubMed: 19153578]
45. Leroy K, Duyckaerts C, Bovekamp L, et al. Increase of adenomatous polyposis coli immunoreactivity is a marker of reactive astrocytes in Alzheimer's disease and in other pathological conditions. Acta Neuropathol. 2001; 102:1–10. [PubMed: 11547943]
46. Menn B, Garcia-Verdugo JM, Yaschine C, et al. Origin of oligodendrocytes in the subventricular zone of the adult brain. J Neurosci. 2006; 26:7907–18. [PubMed: 16870736]
47. Parras CM, Galli R, Britz O, et al. Mash1 specifies neurons and oligodendrocytes in the postnatal brain. Embo J. 2004; 23:4495–505. [PubMed: 15496983]
48. Woodhead GJ, Mutch CA, Olson EC, et al. Cell-autonomous beta-catenin signaling regulates cortical precursor proliferation. J Neurosci. 2006; 26:12620–30. [PubMed: 17135424]
49. Adachi K, Mirzadeh Z, Sakaguchi M, et al. Beta-catenin signaling promotes proliferation of progenitor cells in the adult mouse subventricular zone. Stem Cells. 2007; 25:2827–36. [PubMed: 17673525]
50. Israsena N, Hu M, Fu W, et al. The presence of FGF2 signaling determines whether beta-catenin exerts effects on proliferation or neuronal differentiation of neural stem cells. Dev Biol. 2004; 268:220–31. [PubMed: 15031118]
51. Qu Q, Sun G, Li W, et al. Orphan nuclear receptor TLX activates Wnt/beta-catenin signalling to stimulate neural stem cell proliferation and self-renewal. Nat Cell Biol. 2010; 12:31–40. 1–9. [PubMed: 20010817]
52. Chenn A, Walsh CA. Regulation of cerebral cortical size by control of cell cycle exit in neural precursors. Science. 2002; 297:365–9. [PubMed: 12130776]
53. Zechner D, Fujita Y, Hulsken J, et al. beta-Catenin signals regulate cell growth and the balance between progenitor cell expansion and differentiation in the nervous system. Dev Biol. 2003; 258:406–18. [PubMed: 12798297]
54. Fodde R, Kuipers J, Rosenberg C, et al. Mutations in the APC tumour suppressor gene cause chromosomal instability. Nat Cell Biol. 2001; 3:433–8. [PubMed: 11283620]
55. Kaplan KB, Burds AA, Swedlow JR, et al. A role for the Adenomatous Polyposis Coli protein in chromosome segregation. Nat Cell Biol. 2001; 3:429–32. [PubMed: 11283619]
56. Gounari F, Chang R, Cowan J, et al. Loss of adenomatous polyposis coli gene function disrupts thymic development. Nat Immunol. 2005; 6:800–9. [PubMed: 16025118]
57. Qian Z, Chen L, Fernald AA, et al. A critical role for Apc in hematopoietic stem and progenitor cell survival. J Exp Med. 2008; 205:2163–75. [PubMed: 18725524]

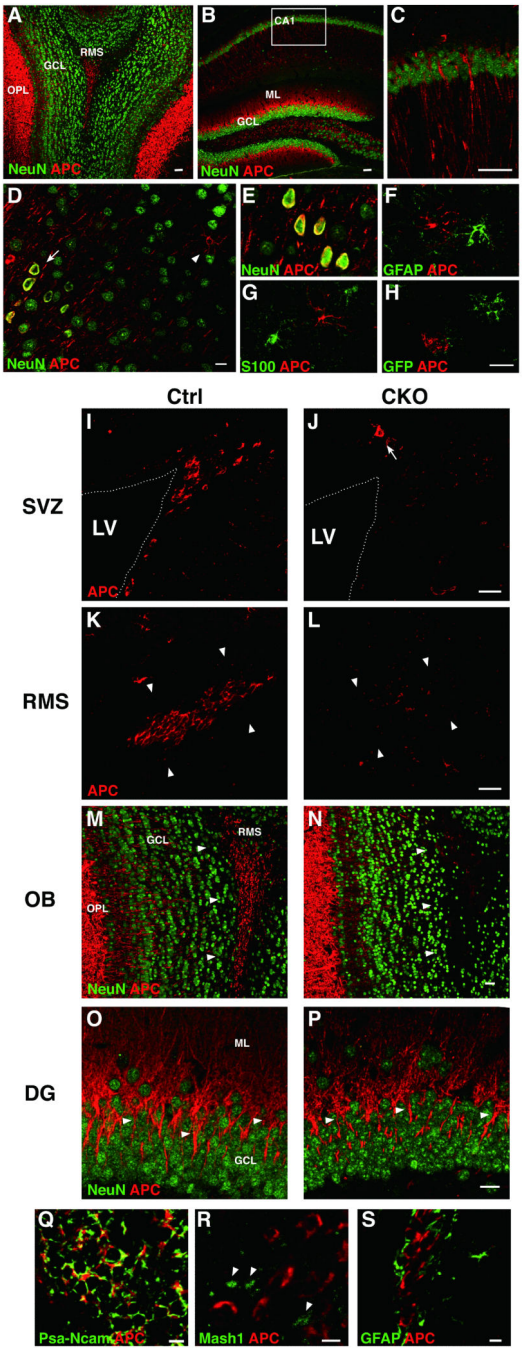

Figure 1.

APC expression in the adult mouse forebrain. APC-immunoreactivity (-IR) is enriched in the OB-OPL (*A*), the axons/dendrites of CA1 pyramidal neurons (*B*, *C*) and the somata of cortical neurons (*arrow in D*, *E*). APC-IR is also observed in the cells extending fine processes (*arrowhead in D*) that are negative for astrocyte markers S100 and GFAP as well as the reporter GFP (*F-H*). In the adult neurogenic regions of control mice, APC-IR is prominent in the cells in the SVZ (*I*), RMS (*arrowhead in K*) and OB-RMS (*arrowhead in M*) as well as the granule cell dendrites of the DG (*arrowhead in O*). APC-IR is markedly

reduced in the SVZ, RMS, and OB-RMS of CKO mice (*J*, *L*, *N*). Note that APC-IR in the cells with fine processes (*arrow in J*) as well as that in the OB-OPL is preserved. APC-IR is colocalized with PSA-NCAM$^+$ neuroblasts but not Mash1$^+$ (*arrowhead*) and GFAP$^+$ cells in control mice (*Q*-*S*). Scale bars: A-C, 40 μm; D-H, 10 μm; I-P, 20 μm; Q-S, 5 μm. OPL, outer plexiform layer; Ctrl, controls; GCL, granule cell layer; RMS, rostral migratory stream; SVZ, subventricular zone; LV, lateral ventricle; OB, olfactory bulb; DG, hippocampal dentate gyrus.

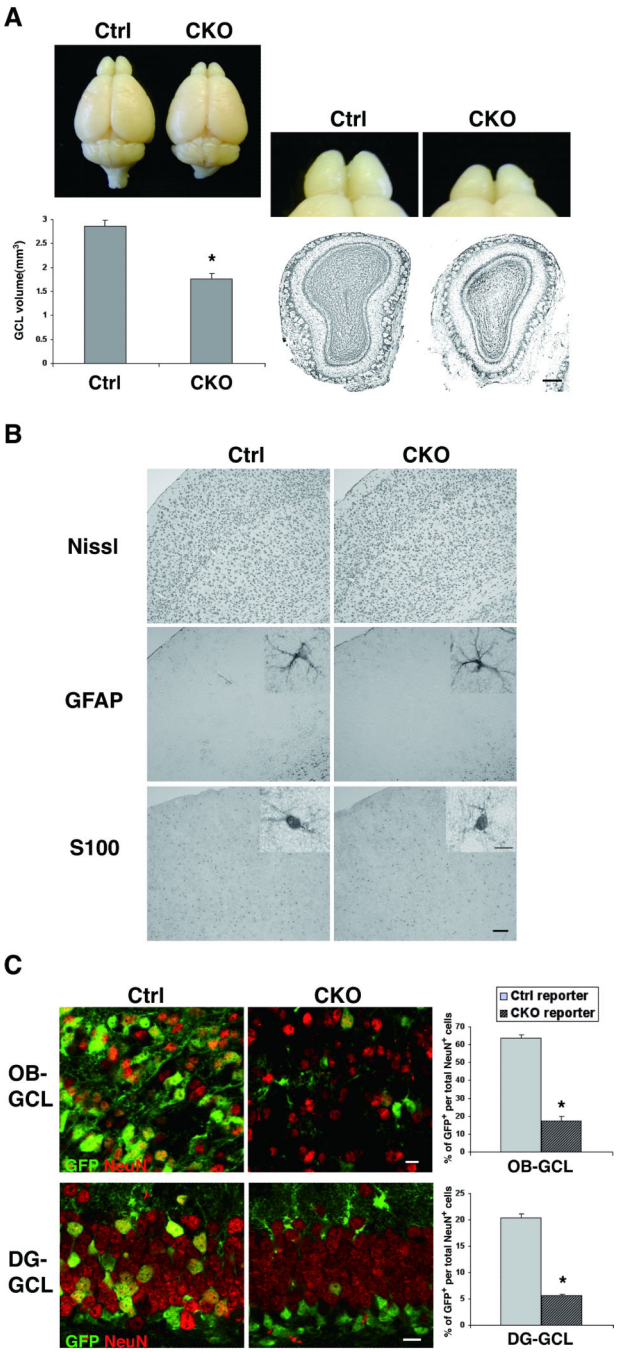

Figure 2.

Marked reduction of GFAP$^+$ NSC-derived neurogenesis in APC-CKO mice. *A.* Representative pictures of the brains and Nissl-stained OB sections show that the OB is shrunken in adult CKO mice. The volume of the GCL significantly decreased in CKO mice compared to controls. n=5, *p<0.001 versus controls, t test. *B.* Nissl-stained sections show that the cortical architecture is normal in CKO mice. The distribution and morphology (*inset*) of GFAP$^+$ and S100$^+$ astrocytes are indistinguishable between CKO and control mice. *C.* The proportions of the reporter GFP$^+$ neurons per total neurons in the OB-GCL and

in the DG-GCL of CKO reporter mice were significantly reduced compared to those of control reporter mice. n=3-4, *p<0.001 versus controls, t test. Scale bars: A, 100 μm; B, 50 μm; B (inset), C, 10 μm. GCL, granule cell layer; OB, olfactory bulb; DG, hippocampal dentate gyrus.

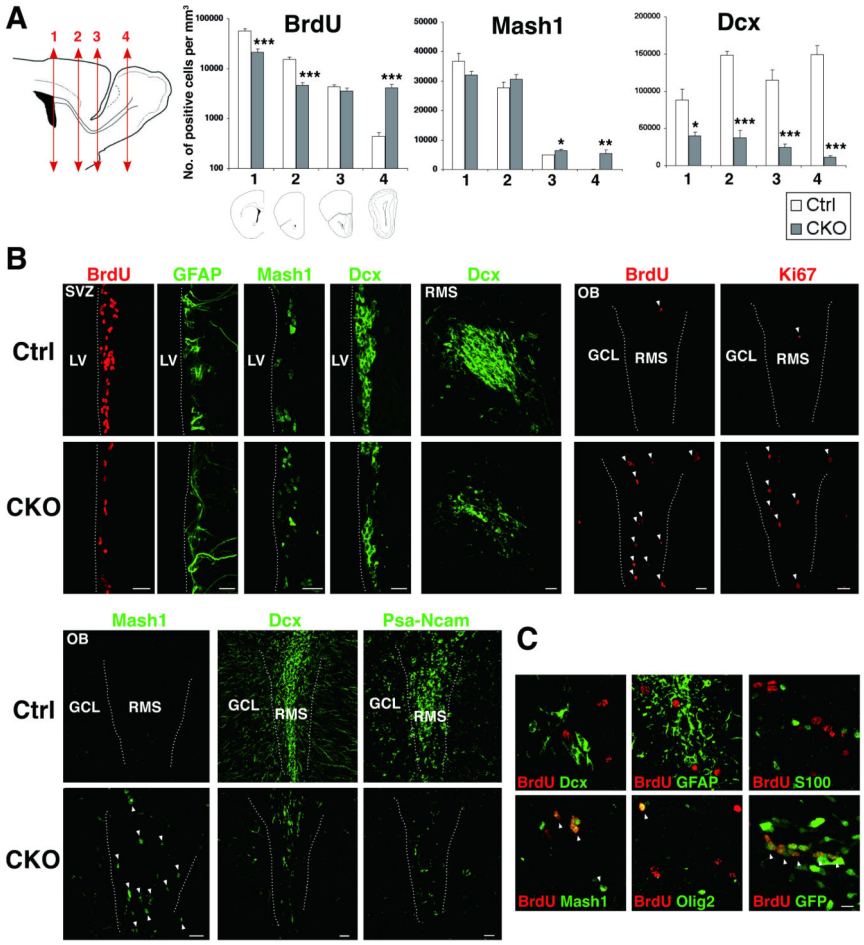

Figure 3.

Depletion of neuroblasts with a concomitant increase in dividing Mash1$^+$ cells in the OB of APC-CKO mice. *A.* Quantification of BrdU$^+$ dividing cells (administered 2 h before tissue harvest), Mash1$^+$ cells, and Dcx$^+$ neuroblasts through the SVZ-RMS. Scheme illustrating coronal sections at different rostrocaudal levels used for quantification; the anterior SVZ(*1*), caudal RMS(*2*), rostral RMS(*3*), and OB-RMS(*4*). n=4-7, **p*<0.05, ***p*<0.01, ****p*<0.001 versus controls, *t* test. *B,* Representative images of coronal sections of the SVZ and OB stained by BrdU, Ki67, GFAP, Mash1, Dcx, and PSA-NCAM. Note that BrdU$^+$ and Ki67$^+$ dividing cells as well as Mash1$^+$ cells markedly increase, whereas Dcx$^+$ and PSA-NCAM$^+$ neuroblasts are depleted in the OB of CKO mice. *C.* BrdU$^+$ dividing cells in the OB of CKO mice are frequently positive for GFP and Mash1, and occasionally positive for Olig2 (*arrowhead*), but negative for Dcx, GFAP, and S100. Scale bars: B, 20 μm; C, 10 μm. SVZ, subventricular zone; RMS, rostral migratory stream; OB, olfactory bulb; GCL, granule cell layer, LV, lateral ventricle; Dcx, doublecortin.

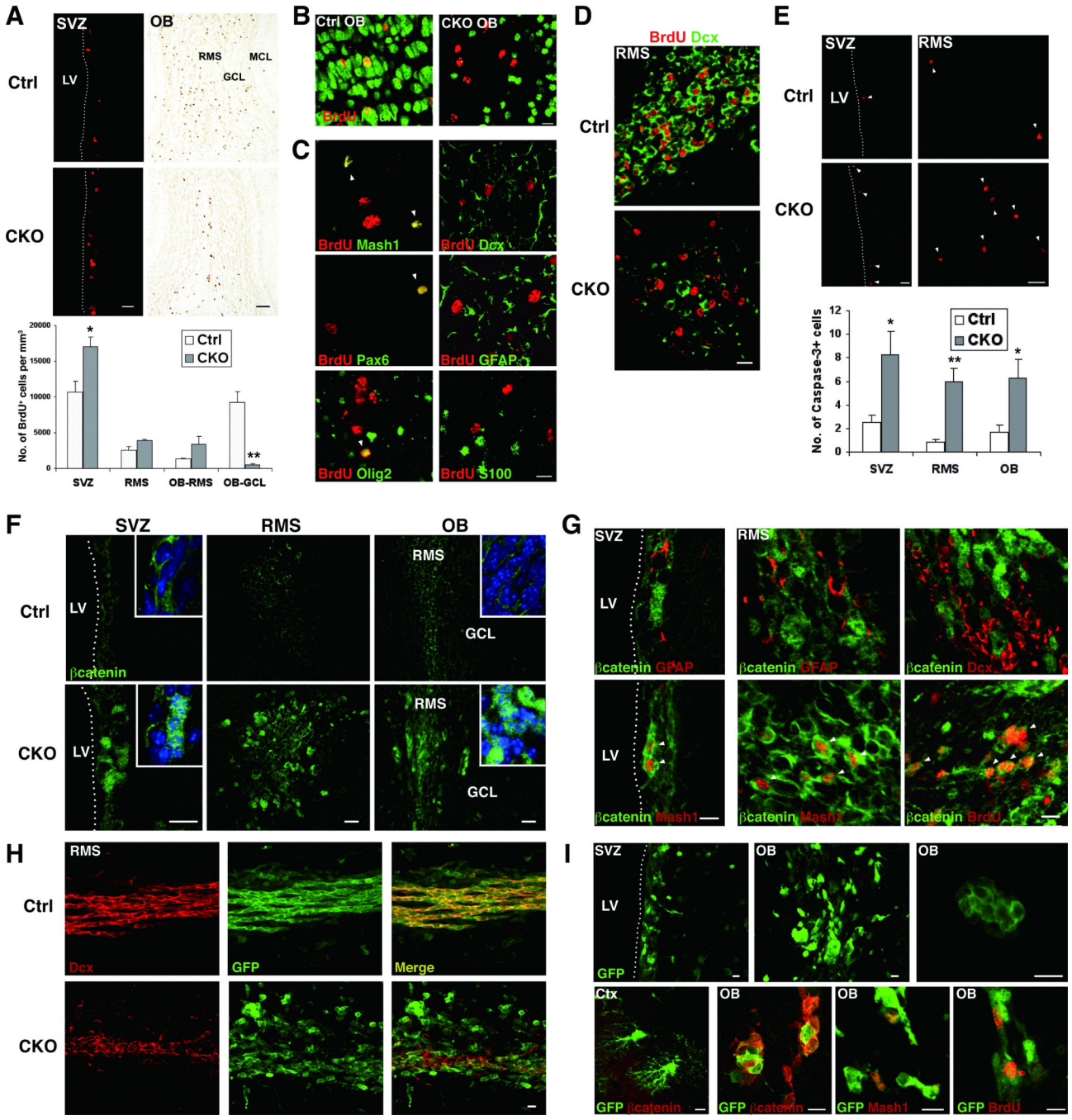

Figure 4.

Fate of newly generated cells and accumulation of beta-catenin in APC-CKO mice. *A.* The majority of long-term BrdU-retaining cells (14 d) locate in the OB-GCL in control mice, whereas many $BrdU^+$ cells still remain in the SVZ, caudal RMS, and OB-RMS in CKO mice. n=4-5, *$p<0.05$, **$p<0.01$, versus controls, *t* test. *B.* Double immunofluorescence staining for BrdU and mature neuronal marker NeuN. *C.* Double immunofluorescence staining for BrdU and mature and immature cell markers in the OB-RMS of CKO mice. *D.* Double immunofluorescence staining for BrdU (48 h) and Dcx. *E.* The number of

caspase-3$^+$ apoptotic cells (*arrowhead*) was significantly higher in CKO mice. n=4, *p<0.05, **p<0.01, versus controls, *t* test. *F*. Beta-catenin expression in control and CKO mice. Nuclei are counterstained with TOPRO-3 (inset, *blue*). *G*. Beta-catenin$^+$ cells in CKO mice are negative for GFAP and Dcx, but frequently positive for Mash1 and BrdU (2 hr) (*arrowhead*). *H*. In the RMS of control reporter mice, GFP$^+$ are orderly arranged in a caudorostral orientation and positive for Dcx. In CKO reporter mice, many GFP$^+$ cells are negative for Dcx and form small cell aggregates. *I*. GFP$^+$ cell aggregates are composed of tightly packed Mash1$^+$ and BrdU$^+$ cells with beta-catenin accumulation. Note that cortical astrocytes express GFP but do not accumulate beta-catenin (*lower left panel*). Scale bars: A (SVZ), 20 μm; A (OB), 100 μm; B, C, D, 10 μm; E, F, 20 μm, G, H, I, 10 μm. SVZ, subventricular zone; LV, lateral ventricle; OB, olfactory bulb; ML, mitral cell layer; GCL, granule cell layer; RMS, rostral migratory stream; Ctx, cortex; Dcx, doublecortin.

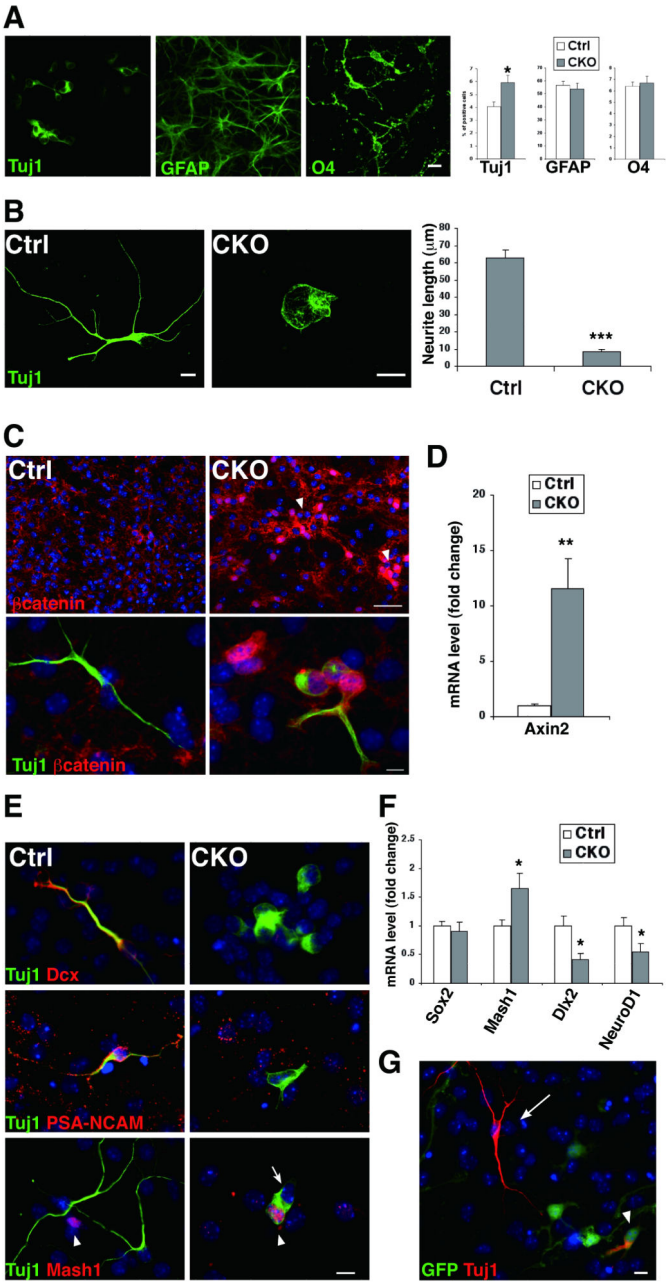

Figure 5.

Impaired neuronal differentiation of APC-deficient cells *in vitro*. *A.* CKO neurospheres generated significantly higher number of Tuj1$^+$ cells, but these cells were morphologically abnormal with very short neurites. The number and morphology of GFAP$^+$ and O4$^+$ glia were indistinguishable between control and CKO cultures. *p<0.05, versus controls, *t* test. n=6 separate experiments per conditions. *B.* The mean length of the longest neurite per neurons was more than seven times shorter in CKO cells. ***p<0.001 versus controls, *t* test. *C.* Tuj1$^+$ cells in CKO cultures are frequently clustered (*arrowhead*) with nuclear accumulation of beta-catenin. *D.* Quantitative RT-PCR analysis showed that the expression of Axin-2 mRNA markedly increased in CKO cultures. **p<0.01, *t* test. n=4. *E.* Tuj1$^+$ cells

and Mash1^{+} cells (*arrowhead*) are mutually exclusive in control cultures. Tuj1^{+} cells in CKO cultures are mostly negative for Dcx and PSA-NCAM, but occasionally positive for Mash1 (*arrowhead*) and form a tight cluster with Mash1^{-} cells (*arrow*). *F*. The expression of Mash1 mRNA increased but that of Dlx2 and NeuroD1 mRNA decreased. *p<0.05, *t* test. n= 6. *G*. GFP^{-} wild-type cells failed to rescue impaired neuronal differentiation of GFP^{+} CKO cells (*arrowhead*) in mixed cultures. The image shown is representative of three independent experiments. Note that GFP^{-} wild-type neurons (*arrow*) are morphologically normal. Nuclei are stained with DAPI (*blue*). Scale bars: A, B, C (lower panels), E, G, 10 μm; C (upper panels), 50 μm; Dcx, doublecortin.

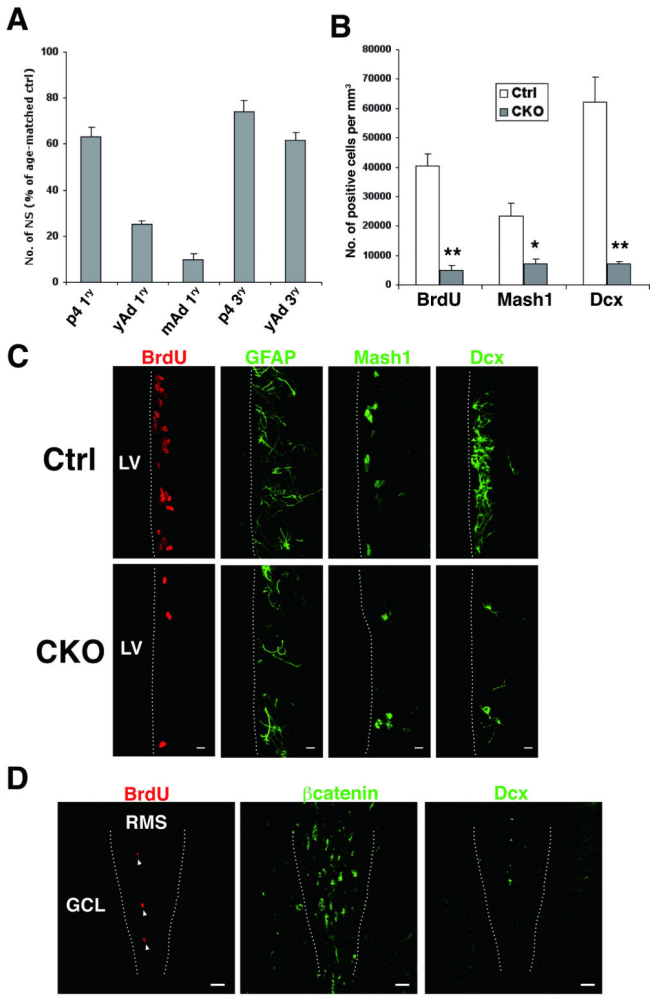

Figure 6.

The subventricular germinal zone is exhausted in APC-CKO mice with age. *A.* The yields of primary neurospheres recovered from postnatal day 4 (*P4*), young adult (8-12w, *yAd*), and middle-aged (6-7 months, *mAd*) CKO mouse periventricular zones progressively decreased with age (63%, 25%, and 9% of controls at P4, yAd, and mAd, respectively. $p<0.001$ versus controls, *t* test.). The yields of tertiary neurospheres improved but still significantly decreased (74% and 62% of controls at P4 and yAd, respectively. $p<0.001$ versus controls, *t* test.). The number of neurospheres in CKO cultures was shown as a proportion to that in the cultures from age-matched littermate controls. n=6-8 separate experiments per conditions. *B.* Quantification of $BrdU^+$ dividing cells (2 h), $Mash1^+$ cells, and Dcx^+ neuroblasts in the SVZ of middle-aged mice. n=3, $*p<0.05$, $**p<0.01$, versus controls, *t* test. *C.* In addition to the obvious reduction of $BrdU^+$, $Mash1^+$, and Dcx^+ cells, GFAP-immunoreactivity moderately decreases in the SVZ of middle-aged CKO mice. *D.* Accumulation of beta-catenin and the presence of $BrdU^+$ dividing cells (*arrowhead*) become inconspicuous in the OB of middle-aged CKO mice, whereas the depletion of Dcx^+ cells is remarkable. Scale bars: C, 10 μm; D, 40 μm. SVZ, subventricular zone; LV, lateral ventricle; OB, olfactory bulb; GCL, granule cell layer; RMS, rostral migratory stream; Dcx, doublecortin.

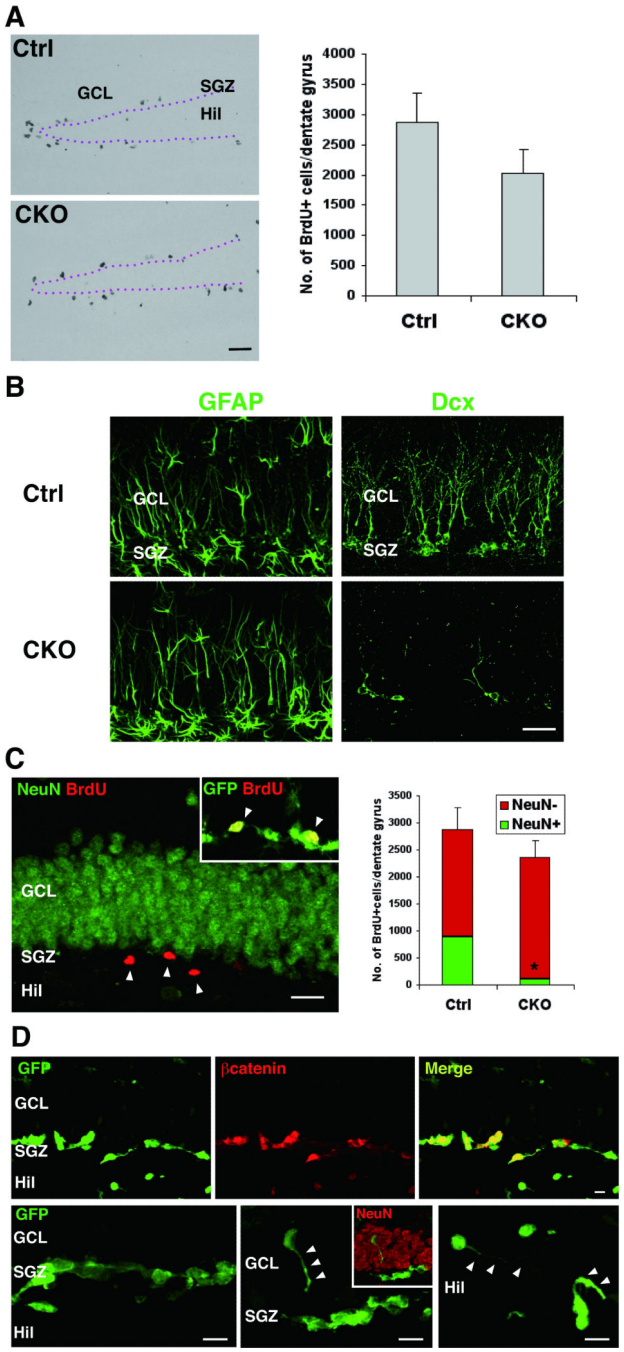

Figure 7.

Reduction of hippocampal neurogenesis with relatively spared cell proliferation. *A.* The mean number of BrdU$^+$ dividing cells (2 hr) modestly decreased in the DG of young adult CKO mice, but the difference is not statistically significant (n=6, p=0.19 versus controls, *t* test.). *B.* GFAP$^+$ radial cells are comparable but Dcx$^+$ neuroblasts markedly decrease in the DG of CKO mice. *C.* Fate of newly generated cells in CKO mice. Long-term BrdU-retaining cells (14 d) remain in the SGZ (*arrowhead*) and negative for NeuN but positive for GFP (*inset*). The total number of BrdU$^+$ cells was not significantly different but that of

BrdU$^+$NeuN$^+$ cells significantly decreased. n=4, *p<0.01 versus controls, *t* test. *D.* GFP$^+$ cells in the SGZ of CKO reporter mice accumulate beta-catenin (*upper panels*). Most of GFP$^+$ cells in the SGZ are tightly clustered (*left lower panel*), whereas a few isolated GFP$^+$ cells identified in the GCL (*middle lower panel*) and hilus (*right lower panel*) extend randomly oriented processes (*arrowhead*). Scale bars: A, 100 μm; B, C, 20 μm; D, 10 μm. DG, dentate gyrus; GCL, granule cell layer; SGZ, subgranular zone; Hil, hilus; Dcx, doublecortin.